Discussiones Mathematicae
Graph Theory 38 (2018) 405–427
doi:10.7151/dmgt.2021

A LIMIT CONJECTURE ON THE NUMBER OF HAMILTONIAN CYCLES ON THIN TRIANGULAR GRID CYLINDER GRAPHS [1]

Olga Bodroža-Pantić

Faculty of Sciences, Department of Mathematics and Informatics
University of Novi Sad, Novi Sad, Serbia

e-mail: olga.bodroza-pantic@dmi.uns.ac.rs

Harris Kwong

SUNY at Fredonia, Department of Mathematical Sciences
Fredonia, NY 14063, USA

e-mail: kwong@fredonia.edu

Rade Doroslovački

Faculty of Technical Sciences
University of Novi Sad, Novi Sad, Serbia

e-mail: ftndean@uns.ac.rs

and

Milan Pantić

Faculty of Sciences, Department of Physics
University of Novi Sad, Novi Sad, Serbia

e-mail: mpantic@df.uns.ac.rs

Abstract

We continue our research in the enumeration of Hamiltonian cycles (HCs) on thin cylinder grid graphs $C_m \times P_{n+1}$ by studying a triangular variant of the problem. There are two types of HCs, distinguished by whether they wrap around the cylinder. Using two characterizations of these HCs, we prove that, for fixed m, the number of HCs of both types satisfy some linear recurrence relations. For small m, computational results reveal that the two

[1] This work was supported by the Ministry of Education and Science of the Republic of Serbia (Grants OI 174018, OI 174026, OI 171009 and III 46005).

numbers are asymptotically the same. We conjecture that this is true for all $m \geq 2$.

Keywords: contractible Hamiltonian cycles, generating functions, thin triangular grid cylinder graph.

2010 Mathematics Subject Classification: Primary 05C30; Secondary 05C50, 05A15.

1. Introduction

A Hamiltonian cycle (HC) on a simple graph is a cycle that visits every vertex exactly once. While it is an intensely studied topic in mathematics, physicists and chemists also find many applications of Hamiltonian cycles in their own fields of study, especially in polymer physics, which refer to the protein folding problem and a mathematical idealization of polymer melts (see [1] or [8] and references in them for a brief overview). For example, the number of Hamiltonian cycles on a graph corresponds to the entropy of a polymer system. The entropy per site is

$$\frac{S}{N} = \frac{1}{N} \ln C_{N,P},$$

where $C_{N,P}$ is the number of Hamiltonian cycles in a N-point lattice with periphery P (see Section 7).

Many efforts have been devoted to the enumeration of Hamiltonian cycles and related problems in a rectangular grid graph $P_m \times P_{n+1}$. They are documented in, among others, [1, 4, 7, 8, 10, 13, 14, 15, 19, 20]. The transfer matrix method [5, 18] provides a powerful tool in this regard. Simply put, for each fixed m, we analyze how a Hamiltonian cycle grows or evolves as n increases. By taking a snapshot of how each column within the Hamiltonian cycle may look like, we compile a list of possible configurations. A transfer matrix is used to record the transition between these configurations, which allows us to determine the generating function for the number of Hamiltonian cycles. Since m is fixed, and n increases, we call the underlying graphs "thin" rectangular grids.

We have extended the research in two different directions. By adding a diagonal in every cell within a rectangular grid graph, a triangular grid graph [11, 16] is formed. We studied its enumeration problem in [2]. It is obvious that the analysis is much more involved than that in a rectangular grid. Another direction is to study the thin grid cylinder graph $C_m \times P_{n+1}$. This time, the difficulty arose from the existence of two kinds of Hamiltonian cycles, each with its own distinctive properties. In brief, the first kind perches on or wraps around the cylindrical surface, while the second kind can be viewed as being pasted onto the surface. In topological language, one can call the first ones *non-contractible*

(as Jordan curves) HCs, and the second ones *contractible* HCs (see Figure 1). Our findings were reported in [3].

In contrast to the approach in [1, 10] that encodes the vertices of the grid graph, in this paper and [2, 3], we encode the cells (regions) in the grid graph. Despite the fact that all three research projects utilize the same idea of k-SIST equivalence relation (which was first used in [4] and independently in [19]), the structure of each of these grid graphs calls for separate and different analyzes in each of them.

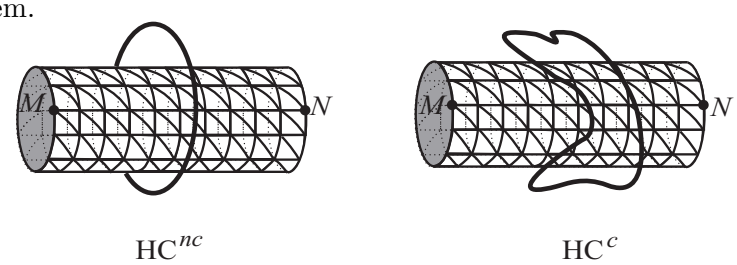

Figure 1. Two types of Hamiltonian cycles that either wrap around or paste over the cylindrical surface.

In this paper, we turn our attention to thin triangular grid cylinder graphs. They are constructed from $C_m \times P_{n+1}$ by adding a diagonal in each of its mn cells. Hence, it is a combination of the two problems mentioned above. We are interested in finding, for each fixed m, the two sequences $\left\{t_m^{nc}(n)\right\}_{n\geq 1}$ and $\left\{t_m^{c}(n)\right\}_{n\geq 1}$, where $t_m^{nc}(n)$ and $t_m^{c}(n)$ denote the number of the two kinds of Hamiltonian cycles. We find that their generating functions share the same denominator. Therefore, we deduce that both sequences satisfy the same linear homogeneous recurrence relation with constant coefficients. For each fixed integer m between 2 and 10 and large enough n, our computational data suggest that $t_m^{nc}(n)$ and $t_m^{c}(n)$ have the same number of digits, and they start with the same sequence of digits. For example, both $t_{10}^{nc}(100)$ and $t_{10}^{c}(100)$ have 317 digits, and their first 42 digits are identical:

$$t_{10}^{nc}(100) = 295413255477398657487606957121168569069871383270437668402046997071327345295037011160679038807631916668443488106395752301860539638798124977023250141880585607555417279066725118755722729324466018114034925704723685759861382100376732544151396294690766637278216200993626745098659675337318451081110455368944549611852805144 12,$$

$$t_{10}^{c}(100) = 295413255477398657487606957121168569069871444691310244546048177794445744048094091315210470101142887573482026898090250982671781264788326018341067718490213351595462908315981369994050584970194195508986614554879420849416039022546437778763645792116174357643016368791135715450583806457384538564345459008648522979200789853 00.$$

It appears that $t_m^{nc}(n) \sim t_m^c(n)$ for each fixed integer m between 2 and 10. This prompts the questions whether it is true for all integers $m \geq 2$, and why is this happening.

2. Preliminaries

The graph $C_m \times P_{n+1}$ can be represented as a rectangular grid cylinder with mn cells. Let its vertices be labeled (i, j), where $1 \leq i \leq m$, and $1 \leq j \leq n+1$. For each $i \leq m$ and $j \leq n$, adding a diagonal that joins the vertex (i, j) to the vertex $((i+1) \bmod m, j+1)$ produces two subregions that we shall call *windows*, as they were referred to in some literature [2, 3, 4]. The window lying above the diagonal is called the *up-window*, and denoted $u_{i,j}$. Likewise, the *down-window* $d_{i,j}$ is the one that lies below the diagonal. If the position is not our primary concern, we will simply denote a window $w_{i,j}$. We call the resulting graph a *triangular grid cylinder graph*, and denote it by $T_{m,n}$. Obviously, each column of $T_{m,n}$ contains $2m$ windows.

We distinguish two types of HCs: those that divide the cylindrical surface (imagine it as being extended indefinitely to both left and right) into two infinite regions, and those that divide the surface into one finite (bounded) and one infinite region (see Figure 1). The first type wraps around the cylindrical surface, hence divides the cylindrical surface into the left half and the right half, it resembles a bracelet around an arm. The second type encloses a finite region (the interior region) and leaves an infinite region on the outside. One could imagine it being pasted onto the cylindrical surface. Geometrically, the second kind can be contracted, but the first kind cannot. Hence, we call them *type NC* and *type C*, and, abbreviate them as HC^{nc} and HC^{c}, respectively. We use $t_m^{nc}(n)$ and $t_m^c(n)$ to indicate the number of HC^{nc}s and HC^{c}s. Their respective generating functions are written as $\mathcal{T}_m^{nc}(x)$ and $\mathcal{T}_m^c(x)$.

Here is an another way to look at the differences between these two types of HCs. Let us "cut open" the cylindrical surface of $T_{m,n}$ along the line MN (see Figure 1), then "flatten" it and line up infinitely many copies of the obtained picture of our graph as shown in Figure 2. By doing so we form an infinite triangular lattice of width n. The subgraph of it produced from a HC^{nc} (Figure 2 left) represents an infinite broken line (curve consisting of countably many connected line segments) which divides the plane into two regions: one on the left, the other on the right, of the HC. We call them the *zero region* and the *positive region*, respectively. In the case of a HC^{c} (Figure 2 right), the subgraph consists of countably many closed polygonal lines on the plane. Each polygon encloses a region that we shall call the *positive region*, and the region outside the polygons will be called the *zero region*. The region on the cylindrical surface determined by the HC under consideration is called *positive* (respectively *zero*) *region* if and

only if it corresponds to the positive (respectively zero) region/regions in the flat surface.

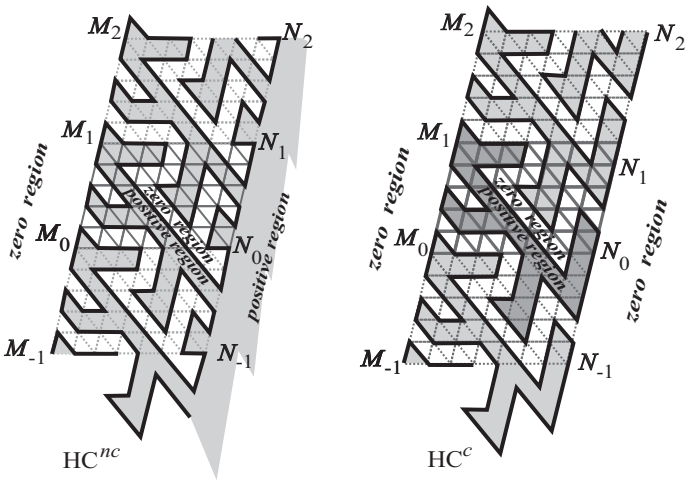

Figure 2. Products of flattening and replication.

To distinguish one HC from another, we encode the windows with 0 and 1, in the following manner. For a HC^{nc}, the 1-windows are those in the positive region (the region on the right of the HC), and the 0-windows are those in the zero region (the one on the left of the HC). See Figure 3. For a HC^{c}, the windows in the positive (interior) region are the 1-windows, those outside are the 0-windows. For a reason that will become clear, we also call the 1-windows *positive windows*.

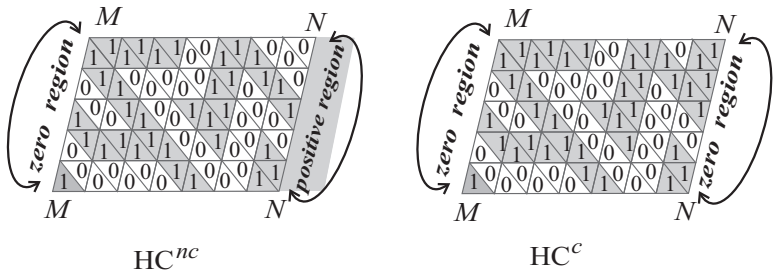

Figure 3. The first characterization of HC^{nc} and HC^{c}.

A Hamiltonian cycle is the boundary of regions, each of which consists of windows of the same type. This observation suggests that we could study the dual graph of $T_{m,n}$. The dual graph $W_{m,n}$ comprises of vertices corresponding to the windows of $T_{m,n}$, and two vertices in the dual are adjacent if their respective

windows in $T_{m,n}$ share a common edge (see Figure 4). The vertices in $W_{m,n}$ are also labeled as $u_{i,j}$ and $d_{i,j}$, and, in general, $w_{i,j}$ if we disregard its position.

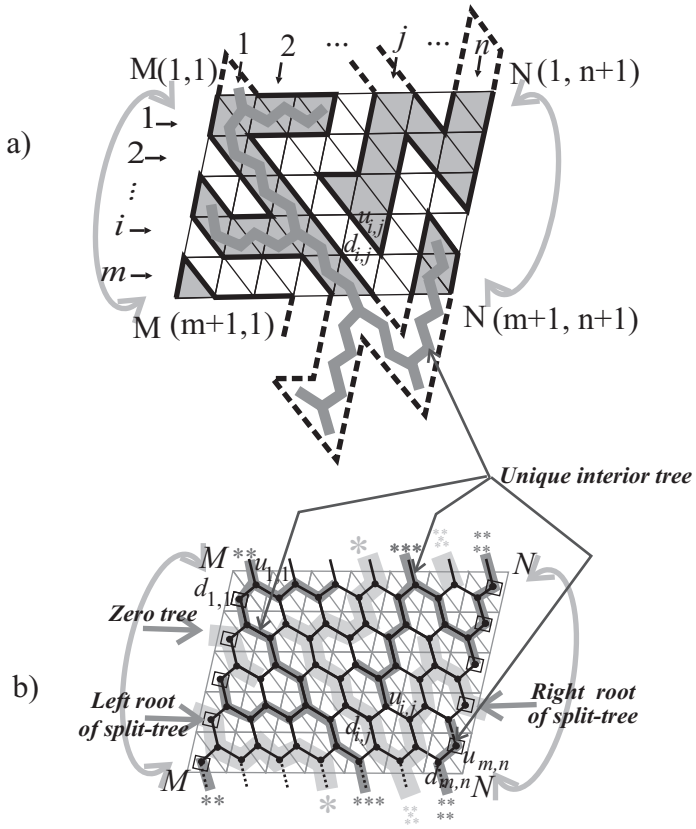

Figure 4. a) A Hamiltonian cycle of type C on $T_{5,7}$. Notice how it is "pasted" onto the grid cylinder. b) The unique interior tree for the HC^c in the dual graph $W_{5,7}$ is colored dark gray. The exterior forest is in light gray. Only one ET (the split tree) has both left and right roots.

The vertices in $W_{m,n}$ are called 0- and 1-vertices, depending on whether they represent 0- or 1-windows in $T_{m,n}$. The 1-vertices in $W_{m,n}$ form a forest of *positive trees* (PTs). In the case of a HC^c, the forest has only one component. Since it is found in the interior of the HC, we also call it the *interior tree*. Note that, in contrast, the forest formed by 1-vertices on a HC^{nc} may have more than just one component, but that every such tree has exactly one vertex corresponding to an up-window from the last column. We call that vertex the *right root* of this tree. The 0-vertices form a forest of *zero trees* (ZTs) for both types of HCs. For a HC^{nc}, every zero tree has exactly one vertex corresponding to a down-window

from the first column. We call it the *left root*. For example, the HC^{nc} in Figure 3 has two zero trees with left roots $d_{2,1}$ and $d_{4,1}$, and two positive trees with right roots $u_{3,7}$, and $u_{5,7}$.

For a HC^c, we also call the zero trees its *exterior trees* (abbreviated ETs). An up-window in the first column belonging to an ET is called its *left root*. Similarly, a down-window in the last column belonging to an ET is called its *right root*.

Because a HC^c has only one exterior region (which extends to both left and right sides of $T_{m,n}$ on the cylindrical surface) and only one interior (bounded) region, there is exactly one ET with both left and right roots. We call it the *split tree* of the HC. Every ET different from a split tree has either exactly one left root and no right roots or exactly one right root and no left roots. For example, the HC^c in Figure 3 has a split tree with the left root $d_{4,1}$ and the right root $u_{4,7}$, and one ET with the left root $d_{2,1}$.

Let $t_m(n)$ be the number of HCs in $T_{m,n}$, where $n \geq 1$. Obviously, $t_m(n) = t_m^{nc}(n) + t_m^c(n)$ for each $n \geq 1$. Our main objective is to find the generating function $\mathcal{T}_m(x) = \sum_{n\geq 0} t_m(n+1)x^n$, which is the sum of the generating functions $\mathcal{T}_m^{nc}(x) = \sum_{n\geq 0} t_m^{nc}(n+1)x^n$ and $\mathcal{T}_m^c(x) = \sum_{n\geq 0} t_m^c(n+1)x^n$.

In the next two sections, we describe two different methods of characterizing Hamiltonian cycles. In Section 5, we discuss how to use the second characterization to obtain the generating functions. The results are presented in Section 6. In Section 7, we study the asymptotic values of $t_m^c(n)$ and $t_m^{nc}(n)$ as n approaches infinity, and propose an open problem for further investigation.

To facilitate our discussion in Section 4, we need a few more definitions.

Definition. Given a nonnegative integer word $d_1 d_2 \cdots d_{2m}$, its *support* is defined as the word $\bar{d}_1 \bar{d}_2 \cdots \bar{d}_{2m}$, where

$$\bar{d}_i = \begin{cases} 1 & \text{if} \quad d_i > 0, \\ 0 & \text{if} \quad d_i = 0. \end{cases}$$

The *support* of a nonnegative integer matrix $[d_{i,j}]$ is defined in a similar manner.

Definition. The subword u of a word v is called a *b-factor* if it is a block of consecutive letters all of which equal to b. A b-factor of v is said to be *maximal* if it is not a proper factor of another b-factor of v.

3. First Characterization of HC

Any fixed HC on $T_{m,n}$ induces an encoding of its $2mn$ cells with 0 and 1 (see Figure 3). We can summarize the encoding with a $(0,1)$-matrix $A = [a^*_{i,j}]_{2m\times n}$, where

$$a^*_{i,j} = \begin{cases} a^u_{\lceil i/2 \rceil, j} & \text{if} \quad i \ \text{ is odd}, \\ a^d_{\lceil i/2 \rceil, j} & \text{if} \quad i \ \text{ is even}, \end{cases}$$

such that $a^d_{i,j}$ and $a^u_{i,j}$ are 0 or 1, depending on whether the respective windows $d_{i,j}$ and $u_{i,j}$ are 0- or 1-windows. For the sake of brevity, we encode the jth column as a binary word $a^u_{1,j}a^d_{1,j}a^u_{2,j}a^d_{2,j}\cdots a^u_{m,j}a^d_{m,j}$. The following result (in which we adopt the convention $a^*_{m+1,j} = a^*_{1,j}$) is easy to verify.

Theorem 1. *The matrix $A = [a^*_{i,j}]_{2m\times n}$ satisfies the following conditions.*

A1. *The* first column (FC) *condition: For $1 \le i \le m$, if $a^d_{i,1} = a^d_{i+1,1}$, then $a^u_{i+1,1} = 1$.*

A2. *The* hexagonal neighborhood (HN) *condition: For $1 \le i \le m$ and $1 \le j < n$, the binary cyclic word $a^d_{i,j}a^u_{i,j}a^d_{i,j+1}a^u_{i+1,j+1}a^d_{i+1,j+1}a^u_{i+1,j}$ formed by the six windows around the vertex $(i+1, j+1)$ (which are represented by a hexagon in $W_{m,n}$) contains exactly one sequence of consecutive 0s and exactly one sequence of consecutive 1s.*

A3. *The* Tree-Root (TR) *condition: The subgraphs of $W_{m,n}$ induced by the 1-vertices form a forest and*

- *For type* NC: *Every positive tree has exactly one up window in the last column of $W_{m,n}$.*
- *For type* C: *There is exactly one positive tree.*

A4. *The* last column (LC) *condition:*

- *For type* NC: *For $1 \le i \le m$, if $a^u_{i,n} = a^u_{i+1,n}$, then $a^d_{i,n} = 0$.*
- *For type* C: *For $1 \le i \le m$, if $a^u_{i,n} = a^u_{i+1,n}$, then $a^d_{i,n} = 1$.*

It is clear that every HC determines exactly one matrix A described above. More importantly, the converse is also true.

Theorem 2. *Every matrix $A = [a^*_{i,j}]_{2m\times n}$ that satisfies the* FC, HN, TR, *and* LC *conditions determines a unique* HC *in $T_{m,n}$.*

Proof. The 1-windows form a collection of regions whose boundaries, according to the three conditions FC, HN, and LC, produce a 2-factor (that is, a spanning 2-regular subgraph) in $T_{m,n}$. The TR condition asserts that the 2-factor has only one component, hence is a HC, which is uniquely determined by the 1-windows. ■

We note that the TR condition can be replaced by a similar condition on the 0-windows, whose corresponding vertices form a forest in $W_{m,n}$.

A3′. *The* zero tree (ZT) *condition:*

- *For type* NC: *Each component of $W_{m,n}$ induced by 0-windows is a tree with exactly one down-window from the first column of $W_{m,n}$ (the root of the* ZT*).*
- *For type* C: *Each component of $W_{m,n}$ induced by 0-windows is a tree (an exterior tree) with exactly one window that is either an up-window from*

the last column of $W_{m,n}$ or a down-window from the first column of $W_{m,n}$ (the root of the ET*) except for the unique tree (split tree) that has both unique up-window from the last column of $W_{m,n}$ and unique down-window from the first column of $W_{m,n}$.*

4. Second Characterization of HC

There are only a limited number of possible configurations that a column within a HC^{nc} or HC^{c} can take on. The characterization of HCs to be introduced in this section allows us to encode the columns of $T_{m,n}$ for any HC^{nc} or HC^{c} in a way that the connections between $t_m^{nc}(n)$ and $t_m^{nc}(n+1)$, or $t_m^{c}(n)$ and $t_m^{c}(n+1)$, can be obtained by studying the transfer matrix relating the configurations that could possibly occur. This leads to the generating functions $\mathcal{T}_m^{nc}(x)$ and $\mathcal{T}_m^{c}(x)$, and consequently the recurrence relation for $t_m^{nc}(n)$ and $t_m^{c}(n)$.

In a way, we are observing how a HC develops, one column at a time, from left to right. The first k columns in a partially formed HC tell us what could happen in the next column, the $(k+1)$st column. By analyzing the number of ways a HC can grow from the first column to the last column, we are able to enumerate them. In this regard, the characterization in Section 3 does not provide an effective tool for enumeration. Whether two columns are adjacent depends not only on their configurations, but also the columns before them.

From the perspective of $W_{m,n}$, the 1-vertices form a union of the trees with right roots in the case of a HC^{nc}, or a tree in the case of a HC^{c}. The 1-vertices in the first k columns form a forest. On a HC^{c}, this forest may not evolve into a tree until the very last column. Hence, some of the 1-vertices in the first j columns that appear to be disconnected may become connected later in column ℓ for some integer $\ell > j$. This prompts us to define the notion of two 1-windows being k-joined.

Definition. Two 1-windows $w_{i,r}$ and $w_{j,s}$ in $T_{m,n}$ (likewise, two 1-vertices in $W_{m,n}$), where $r, s \leq k$, are said to be *joined at the kth column*, or simply *k-joined*, if their corresponding vertices in $W_{m,n}$ belong to the same component in the subgraph formed by the 1-vertices in the first k columns.

For example, in Figure 4a, the windows $u_{1,1}$ and $d_{3,1}$ are 3-joined but not 1-joined and 2-joined, and the windows $u_{3,4}$ and $d_{4,4}$ are 5-joined but not 4-joined. It is obvious that if two windows are k-joined, then they are ℓ-joined for any $\ell \geq k$.

Within a HC, for each fixed k, being k-joined is an equivalence relation on the set of 1-windows in the first k columns, and it has at most m equivalence classes. For example, in Figure 5 left, within column 2, the relation 2-joined

has two equivalence classes. We number these equivalence classes, from top to bottom, $2, 3, \ldots$. Accordingly, we can label the 1-windows within a column of a HC with these numbers to indicate the component they belong to. Call the new labels $b^*_{i,j}$. For example, the labels in column 2 for the considered HC^{nc} form the word 2202203300. It has six maximal b-factors, where $b = 2, 0, 2, 0, 3, 0$, respectively.

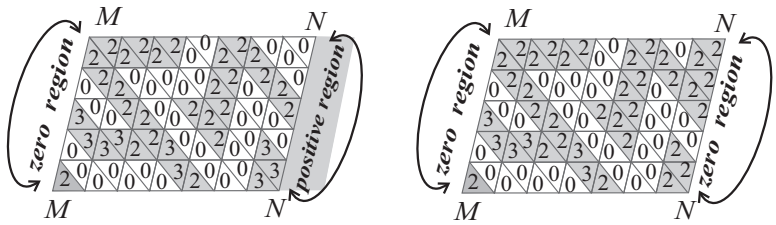

HC^{nc} HC^{c}

Figure 5. The second characterization of HC^{nc} and HC^{c}.

Since the vertices in $W_{m,n}$ are labeled with the alphabet

$$\mathcal{C} = \{0, 2, 3, \ldots, m+1\},$$

a window is said to be a *positive-window* if its label is positive. By replacing the matrix $A = [a^*_{i,j}]_{2m\times n}$ with the matrix $B = [b^*_{i,j}]_{2m\times n}$, we find an alternate characterization of HCs. We adopt the convention $b^*_{m+1,j} = b^*_{1,j}$ and $b^*_{0,j} = b^*_{m,j}$ for $1 \le j \le n$.

Theorem 3. *The matrix $B = [b^*_{i,j}]_{2m\times n}$ satisfies the following properties.*

B1. *The* support matrix (BM) *condition: The support of the matrix, that is, the matrix $A = [a^*_{i,j}]_{2m\times n}$ satisfies conditions* FC, HN, *and* LC.

B2. *The* kth column (KC) *condition: For $1 \le k \le n$, the kth column of B satisfies these subconditions*

(a) *For $1 \le i \le m$, if $b^d_{i,k} > 0$, then $b^u_{i,k}, b^u_{i+1,k} \in \{b^d_{i,k}, 0\}$.*
For $1 \le i \le m$, if $b^u_{i,k} > 0$, then $b^d_{i-1,k}, b^d_{i,k} \in \{b^u_{i,k}, 0\}$.

(b) *The positive letters within any column of B, when read from top to bottom and discarding repetitions, form the sequence $2, 3, \ldots, \ell$ for some integer ℓ.*
For any two different maximal b_1-factor and b_2-factor within the first column of B, where $b_1, b_2 > 0$, we must have $b_1 \ne b_2$.

- *For type* NC: *In the nth column, there is at most one k-factor for each $k > 1$.*

- *For type* C: *The factors in the nth column are either* 0*-factors or* 2*-factors.*

(c) *For $k \geq 2$ and $1 \leq i < j \leq m$, if $b^u_{i,k-1} = b^u_{j,k-1}$, and $a^d_{i,k} = a^d_{j,k} = a^u_{i,k-1} = a^u_{j,k-1} = 1$, then $b^d_{i,k} = b^d_{j,k}$.*

(d) *For $k \geq 2$ and $1 \leq i < j \leq m$, if $b^u_{i,k-1} = b^u_{j,k-1}$, $b^d_{i,k} = b^d_{j,k} = b \in \mathcal{C}^+ = \mathcal{C} \setminus \{0\}$, and $a^u_{i,k-1} = a^d_{i,k} = 1$, then $b^d_{i,k}$ and $b^d_{j,k}$ must appear on two different b-factors.*

(e) *If $k \geq 2$, and if v and u are two different maximal b-factors in the kth column for some $b > 0$, then there is* exactly one *sequence $v = v_1, v_2, \ldots, v_p = u$ of $p > 1$ different maximal b-factors in the kth column which satisfies the following condition: for every i, where $1 \leq i < p$, in the $(k-1)$th column, there exists exactly one letter $b^u_{j_i,k-1}$ with $a^u_{j_i,k-1} = a^d_{j_i,k} = 1$ for which $b^d_{j_i,k} \in v_i$, and there exists exactly one letter $b^u_{s_{i+1},k-1}$ with $a^u_{s_{i+1},k-1} = a^d_{s_{i+1},k} = 1$ for which $b^d_{s_{i+1},k} \in v_{i+1}$ and $b^u_{j_i,k-1} = b^u_{s_{i+1},k-1}$; and $j_i \neq s_i$ for $1 < i < p$.*

(f) *For $k \geq 2$ and for each $b \in \mathcal{C}^+$ that appears in column $k-1$, there exists i, where $1 \leq i \leq m$, for which $b^u_{i,k-1} = b$ and $b^d_{i,k} > 0$.*

(g) *Every column must contain both positive and zero entries.*

Proof. Because of the encoding method we use to construct B, it must satisfy conditions BM and KC(b). The k-joined relation implies that conditions KC(a), KC(c), and KC(e) must be met. The property KC(e) corresponds to the tree property that any two nodes are connected by a unique path. If condition KC(f) is not true, then the subgraph of $W_{m,n}$ induced by the 1-windows would have more than one component (impossible for HC^c) or have a tree without right root (impossible for HC^{nc}). We need condition KC(d) because a cycle will be formed amongst the 1-vertices in $W_{m,n}$ if this is not true. Further, the occurrence of a column with no zero window or with no positive window would imply that the corresponding subgraph in $T_{m,n}$ is not connected, which is impossible. So, the condition KC(g) is valid. ■

Theorem 4. *Every matrix $B = [b^*_{i,j}]_{2m \times n}$ that satisfies the conditions* BM *and* KC *determines a unique* HC *in $T_{m,n}$.*

Proof. It suffices to show that the support of B (which could be either B^{nc} or B^c) satisfies conditions FC, HN, TR and LC in Theorem 1. Since condition BM implies that conditions FC, HN, and LC are met, we only need to show that condition TR is also met. The conditions KC(a) and KC(c) ensure that all the 1-windows in the same column belonging to the same equivalence class of the equivalence relation of being k-joined are labeled by the same number. Properties KC(d) and KC(e) yield the forest structure for the subgraph of $W_{m,n}$

induced by positive windows (since no cycle can occur). The properties KC(f), KC(b) and BM (LC) for type NC Hamiltonian cycles assert that every positive tree in $W_{m,n}$ has exactly one right root. For type C Hamiltonian cycles, the property KC(f) implies that for every positive window there exists a path starting from this window and finishing in the last column of $W_{m,n}$, and the property KC(b) guarantees that the subgraph of $W_{m,n}$ induced by the positive windows is connected. ■

5. Technique for Enumerating Hamiltonian Cycles

Let $m \geq 2$ be a fixed integer. There are only a finite number of integer words $b_1 b_1 \cdots b_{2m}$ from the alphabet $\mathcal{C}$ that may appear in a column within the matrix B. Represent them as vertices of a digraph $\mathcal{D}_m$. Hence, $V(\mathcal{D}_m)$ consists of all the possible columns that may appear within the encoding of any HC. For practical purposes, instead of writing the vertices of $\mathcal{D}_m$ in the form of $(b_1, b_2, \ldots, b_{2m-1}, b_{2m})$, we record them as $(u_1\text{-}d_1, u_2\text{-}d_2, \ldots, u_m\text{-}d_m)$ to emphasize the coding of the up and down windows. Using an argument similar to the one used in [2, 3], we obtain the following bound on $|V(\mathcal{D}_m)|$.

Theorem 5. *Let C_m and M_m denote the mth Catalan and Motzkin number, respectively. Then*

$$|V(\mathcal{D}_m)| \leq 2 \sum_{k=1}^{m} \binom{2m}{2k} C_k = 2(M_{2m} - 1).$$

The directed lines in $\mathcal{D}_m$ are constructed as follows. Join the vertex v to the vertex u if and only if the column represented by v may appear immediately before the column represented by the vertex u in a HC. Consequently, the two words represented by v and u satisfy conditions B1 and B2. The subset of $V(\mathcal{D}_m)$ that consists of all possible first columns in the matrix B is represented by $\mathcal{F}_m$. The subset of $V(\mathcal{D}_m)$ consisting of all possible last columns in the matrix B is denoted $\mathcal{L}_m^{nc}$ or $\mathcal{L}_m^{c}$ depending on whether the HC is of type NC or type C.

The problem of enumerating HC^{nc} or HC^{c} on $T_{m,n}$ now becomes the problem of enumerating oriented walks of length $n-1$ in the digraph $\mathcal{D}_m$ with the initial vertices in the set $\mathcal{F}_m$, and the final vertices in the set $\mathcal{L}_m^{nc}$ or $\mathcal{L}_m^{c}$. We note that Faase [6] used a similar method to enumerate spanning subgraphs of $G \times P_n$ that meet specific conditions.

Because of the rotational symmetry of $T_{m,n}$ and using similar observations like the ones make in [2], we can further simplify the digraph $\mathcal{D}_m$ by identifying

some of its vertices. This produces a multidigraph $\mathcal{D}_m^*$, whose adjacency (transfer) matrix T_m^* is smaller than the original adjacency matrix T_m.

In closing, we would like to remark that there exist other coding schemes for similar problems that are computational more efficient than the ones we propose here. For example, Jensen [9] used a vertex-based coding method. The order of the number of states in Jensen's method is roughly 4^m, while ours is approximately 9^m. Nevertheless, using our method, we are able to enumerate the two types of HCs (HC^{nc} and HC^{c}) separately.

The situation is similar in the enumeration of HCs on triangular grids (graphs obtained from the rectangular grids by adding a diagonal in every window). The theoretic bound for the number of states in [2] (which used window-coding) is expressed in terms of Motzkin's numbers, and the bound in [11] (using vertex-coding) is in terms of Catalan numbers. This makes the theoretic bounds in [2] much higher. However, when we look at the order of the reduced transfer matrix (the order of the reduced multigraph), the numbers of states are comparable, and indeed almost identical. The same can be said when we compare the bounds from [3] and [10] or [1] concerning thin grid cylinder graphs.

6. Computational Results

We implemented the discussion in Section 5 with Pascal programs. Some of the data are collected in Table 1.

m	2	3	4	5	6	7	8	9	10
$\lvert V(\mathcal{D}_m)\rvert$	5	31	169	851	4185	20553	101745	—	—
$\lvert\mathcal{F}_m\rvert$	5	16	49	151	452	1331	3873	—	—
$\lvert\mathcal{L}_m^{nc}\rvert$	5	16	49	151	452	1331	3873	—	—
$\lvert\mathcal{L}_m^{c}\rvert$	4	15	48	150	451	1330	3872	—	—
$\lvert V(\mathcal{D}_m^*)\rvert$	2	5	16	49	177	619	2338	8917	35065
$\lvert\mathcal{F}_m^*\rvert$	2	4	8	16	38	82	194	447	1055
$\lvert\mathcal{L}_m^{nc*}\rvert$	2	3	5	7	13	19	35	59	107
$\lvert\mathcal{L}_m^{c*}\rvert$	1	2	4	6	12	18	34	58	106
order for t_m^{nc} & t_m^{c}	1	4	12	31	83	226	—	—	—
order for t_m	1	2	7	16	43	116	—	—	—

Table 1. The numbers of vertices for the graphs $\mathcal{D}_m$ and $\mathcal{D}_m^*$, the numbers of the first and the last vertices for both types and for both graphs, and the orders of the recurrence relations for t_m^{nc} (and t_m^{c}) and t_m for $2 \le m \le 10$.

Note that $|\mathcal{F}_m| = |\mathcal{L}_m^{nc}| = |\mathcal{L}_m^{c}| + 1$ because we include the isolated vertex

$v^* = (2\text{-}0, 3\text{-}0, \ldots, (m+1)\text{-}0)$ in the set $V(\mathcal{D}_m)$. Although it is used only in the computation of $t_m^{nc}(1)$ and $t_m(1)$, we nevertheless include it in $V(\mathcal{D}_m)$ to simplify our computation. If it is omitted, it is not difficult to establish a bijection between $\mathcal{F}_m \setminus \{v^*\}$ and $\mathcal{L}_m^{nc} \setminus \{v^*\}$, and with $\mathcal{L}_m^{c} \setminus \{v^*\}$.

We adopt the following notations for the generating functions:

$$\mathcal{T}_m^{nc}(x) = \sum_{n=0}^{\infty} t_m^{nc}(n+1)x^n, \qquad \mathcal{T}_m^{c}(x) = \sum_{n=0}^{\infty} t_m^{c}(n+1)x^n,$$

$$\mathcal{T}_m(x) = \mathcal{T}_m^{nc}(x) + \mathcal{T}_m^{c}(x) = \sum_{n=0}^{\infty} t_m(n+1)x^n.$$

Let $q_m^{nc}(x)$, $q_m^{c}(x)$, and $q_m(x)$ denote their denominators, respectively. Note that $q_m^{nc}(x) = q_m^{c}(x)$ because of the common transfer matrix for both types of HCs. Interestingly, for $2 \le m \le 10$, we find that $q_m^{nc}(x)$ is a multiple of $q_m(x)$. Upon further investigation, we conclude that it is helpful to introduce the rational function

$$\mathcal{K}_m(x) = \mathcal{T}_m^{nc}(x) - \mathcal{T}_m^{c}(x),$$

such that

$$\mathcal{T}_m^{nc}(x) = \frac{1}{2}\left(\mathcal{T}_m(x) + \mathcal{K}_m(x)\right), \qquad \mathcal{T}_m^{c}(x) = \frac{1}{2}\left(\mathcal{T}_m(x) - \mathcal{K}_m(x)\right).$$

Since they are rational functions, we can express them as

$$\mathcal{T}_m(x) = \overline{\mathcal{T}}_m(x) + \frac{p_m(x)}{q_m(x)}, \qquad \mathcal{K}_m(x) = \overline{\mathcal{K}}_m(x) + \frac{r_m(x)}{s_m(x)},$$

for some polynomials $\overline{\mathcal{T}}_m(x)$, $\overline{\mathcal{K}}_m(x)$, $p_m(x)$, $q_m(x)$, $r_m(x)$ and $s_m(x)$, where $\deg(p_m) < \deg(q_m)$, and $\deg(r_m) < \deg(s_m)$.

6.1. Thin triangular grid cylinder for $m = 2$

For $n = 2$, $V(\mathcal{D}_2) = \mathcal{F}_2 = \mathcal{L}_2^{nc} = \{v_1, v_2, \ldots, v_5\}$, $\mathcal{L}_2^{c} = \{v_1, v_2, v_3, v_5\}$, $V(\mathcal{D}_2^*) = \mathcal{F}_2 = \mathcal{L}_2^{nc*} = \{v_1, v_4\}$, $\mathcal{L}_2^{c*} = \{v_1\}$, and

$$T_2 = \begin{bmatrix} 1 & 0 & 1 & 0 & 0 \\ 1 & 0 & 1 & 0 & 0 \\ 0 & 1 & 0 & 0 & 1 \\ 0 & 0 & 0 & 0 & 0 \\ 0 & 1 & 0 & 0 & 1 \end{bmatrix}, \qquad \begin{aligned} v_1 &= (0\text{-}0, 2\text{-}2), \\ v_2 &= (0\text{-}2, 2\text{-}0), \\ v_3 &= (2\text{-}0, 0\text{-}2), \\ v_4 &= (2\text{-}0, 3\text{-}0), \\ v_5 &= (2\text{-}2, 0\text{-}0), \end{aligned} \qquad T_2^* = \begin{bmatrix} 2 & 0 \\ 0 & 0 \end{bmatrix}.$$

We find $t_2^{nc}(1) = 5$, $t_2^{c}(1) = 4$, $t_2(1) = 9$, and $t_2^{nc}(n) = t_2^{c}(n) = 2^{n+1}$, for $n \ge 2$. Consequently, $t_2(n) = 2^{n+2}$ for $n \ge 2$. The generating functions are

$$\mathcal{T}_2^{nc}(x) = \frac{5-2x}{1-2x} = 1 + \frac{4}{1-2x}, \qquad \mathcal{T}_2^{c}(x) = \frac{4}{1-2x},$$

$$\mathcal{T}_2(x) = \frac{9-2x}{1-2x} = 1 + \frac{8}{1-2x}, \qquad \mathcal{K}_2(x) = 1.$$

6.2. Thin triangular grid cylinder for $m = 3$

For $n = 3$, we have $V(\mathcal{D}_3^*) = \{v_1, v_2, \ldots, v_5\}$, $\mathcal{F}_3^* = \{v_1, v_2, v_3, v_4\}$, $\mathcal{L}_3^{nc*} = \{v_1, v_2, v_4\}$, $\mathcal{L}_3^{c*} = \{v_3, v_5\}$,

$$\begin{aligned} v_1 &= (0\text{-}0, 0\text{-}2, 2\text{-}2), \\ v_2 &= (0\text{-}0, 2\text{-}0, 3\text{-}3), \\ v_3 &= (0\text{-}0, 2\text{-}2, 2\text{-}2), \\ v_4 &= (2\text{-}0, 3\text{-}0, 4\text{-}0), \\ v_5 &= (0\text{-}0, 2\text{-}2, 0\text{-}2), \end{aligned} \qquad T_3^* = \begin{bmatrix} 2 & 2 & 4 & 0 & 0 \\ 1 & 0 & 2 & 0 & 0 \\ 4 & 0 & 2 & 0 & 2 \\ 0 & 0 & 0 & 0 & 0 \\ 2 & 0 & 1 & 0 & 0 \end{bmatrix}.$$

We find

$$\begin{aligned} \mathcal{T}_3^{nc}(x) &= \frac{2(1-x-x^2)(5+6x+6x^2)}{(1+2x+2x^2)(1-6x-6x^2)} = \frac{8-3x-3x^2}{1-6x-6x^2} + \frac{2+x+x^2}{1+2x+2x^2}, \\ \mathcal{T}_3^{c}(x) &= \frac{6(1+2x)^2}{(1+2x+2x^2)(1-6x-6x^2)} = \frac{8-3x-3x^2}{1-6x-6x^2} - \frac{2+x+x^2}{1+2x+2x^2}, \\ \mathcal{T}_3(x) &= \frac{2(8-3x-3x^2)}{1-6x-6x^2} = 1 + \frac{15}{1-6x-6x^2}, \ \mathcal{K}_3(x) = \frac{2(2+x+x^2)}{1+2x+2x^2} = 1 + \frac{3}{1+2x+2x^2}. \end{aligned}$$

The values of $t_3^{nc}(n)$ and $t_3^{c}(n)$ for $1 \le n \le 12$ are listed in Table 2.

n	$t_3^{nc}(n)$	$t_3^{c}(n)$	$t_3(n)$
1	10	6	16
2	42	48	90
3	318	312	630
4	2160	2160	4320
5	14844	14856	29700
6	102072	102048	204120
7	701448	701472	1402920
8	4821120	4821120	9642240
9	33135504	33135456	66270960
10	227739552	227739648	455479200
11	1565250528	1565250432	3130500960
12	10757940480	10757940480	21515880960

Table 2. The first twelve values of $t_3^{nc}(n)$, $t_3^{c}(n)$, and $t_3(n)$.

6.3. Thin triangular grid cylinder for $m = 4$

For $m = 4$, we find $\mathcal{T}_4(x) = 1 + \frac{p_4(x)}{q_4(x)}$, and $\mathcal{K}_4(x) = 1 + \frac{r_4(x)}{s_4(x)}$, where

$$\begin{aligned} p_4(x) &= 4\left(7 - 10x - 37x^2 - 14x^3 + 12x^4 + 20x^5 + 8x^6\right), \\ q_4(x) &= 1 - 13x - 36x^2 + 26x^3 + 32x^4 + 40x^5 - 8x^6 - 16x^7, \\ r_4(x) &= 4\left(3 - 4x + 9x^2 + 6x^3 - 4x^4\right), \\ s_4(x) &= 1 + 5x + 24x^2 - 6x^3 - 4x^4 + 8x^5. \end{aligned}$$

The first twelve values of $t_4^{nc}(n)$ and $t_4^{c}(n)$ are displayed in Table 3.

n	$t_4^{nc}(n)$	$t_4^{c}(n)$	$t_4(n)$
1	21	8	29
2	124	200	324
3	2600	2472	5072
4	39048	37768	76816
5	581016	590912	1171928
6	8938144	8919016	17857160
7	136155464	136004800	272160264
8	2073272720	2074540392	4147813112
9	31608656296	31605868928	63214525224
10	481716934736	481699387784	963416322520
11	7341358680776	7341520468768	14682879149544
12	111886891169136	111886492907816	223773384076952

Table 3. The first twelve values of $t_4^{nc}(n)$, $t_4^{c}(n)$, and $t_4(n)$.

6.4. Thin triangular grid cylinder for $m = 5$

For $m = 5$, we obtain

$$\mathcal{T}_5(x) = 1 + \frac{p_5(x)}{q_5(x)} \quad \text{and} \quad \mathcal{K}_5(x) = 1 + \frac{r_5(x)}{s_5(x)},$$

where

$$\begin{aligned} p_5(x) = 5(&11 - 15x - 784x^2 - 2881x^3 + 2585x^4 + 23968x^5 + 18106x^6 \\ &- 35922x^7 - 38000x^8 + 7644x^9 - 42856x^{10} + 7728x^{11} \\ &+ 4416x^{12} - 4256x^{13} + 1600x^{14}), \end{aligned}$$

$$
\begin{aligned}
q_5(x) &= 1 - 25x - 280x^2 - 195x^3 + 3471x^4 + 15072x^5 - 11066x^6 - 75742x^7 \\
&\quad - 42208x^8 + 111124x^9 - 26872x^{10} + 52208x^{11} + 39328x^{12} \\
&\quad - 11520x^{13} + 5600x^{14} + 160x^{15} - 1600x^{16}, \\
r_5(x) &= 5(7 - 63x + 418x^2 - 1453x^3 + 3399x^4 - 6568x^5 + 8842x^6 \\
&\quad - 10410x^7 + 9420x^8 - 6956x^9 + 4144x^{10} - 1904x^{11} \\
&\quad + 608x^{12} - 96x^{13}), \\
s_5(x) &= 1 + 3x + 114x^2 - 687x^3 + 2133x^4 - 5012x^5 + 7394x^6 - 11870x^7 \\
&\quad + 11388x^8 - 12684x^9 + 9600x^{10} - 4288x^{11} + 1792x^{12} \\
&\quad - 480x^{13} + 224x^{14} - 160x^{15}.
\end{aligned}
$$

The first twelve values of $t_5^{nc}(n)$ and $t_5^c(n)$ are displayed in Table 4.

n	$t_5^{nc}(n)$	$t_5^c(n)$	$t_5(n)$
1	46	10	56
2	440	860	1300
3	21670	22310	43980
4	763200	696620	1459820
5	24206220	24679200	48885420
6	814333680	819906100	1634239780
7	27386225460	27270802520	54657027980
8	913828130440	914005834580	1827833965020
9	30556142950580	30571254345280	61127397295860
10	1022200379372200	1022046470657460	2044246850029660
11	34182723306352380	34181854253180560	68364577559532940
12	1143123749538226400	1143153291450632580	2286277040988858980

Table 4. The first twelve values of $t_5^{nc}(n)$, $t_5^c(n)$, and $t_5(n)$.

6.5. Thin triangular grid cylinder for $m = 6$

For $m = 5$, we obtain $\mathcal{T}_6(x) = 1 + p_6(x)/q_6(x)$ and $\mathcal{K}_6(x) = 1 + r_6(x)/s_6(x)$, where

$$
\begin{aligned}
p_6(x) &= 109 - 486x - 70398x^2 - 604300x^3 + 3981101x^4 + 47357417x^5 - 40612034x^6 - 1079490063x^7 \\
&\quad + 445126377x^8 + 9733218408x^9 - 26382950380x^{10} - 35367412003x^{11} + 404178532344x^{12} \\
&\quad + 44326233178x^{13} - 2315741889369x^{14} + 429752200895x^{15} + 8946566512706x^{16} \\
&\quad - 4388013042258x^{17} - 28866348311064x^{18} + 21817331539356x^{19} + 64308720113996x^{20} \\
&\quad - 57142690397896x^{21} - 84689046977044x^{22} + 78856910152692x^{23} + 67278727083152x^{24} \\
&\quad - 67734193731296x^{25} - 33596755915712x^{26} + 38399443856480x^{27} + 7518542677696x^{28} \\
&\quad - 11347076361376x^{29} + 118083530848x^{30} + 302884127360x^{31} - 411678931200x^{32} \\
&\quad + 879052011520x^{33} + 66583990016x^{34} - 228599377408x^{35} - 22927906816x^{36} \\
&\quad + 24795945984x^{37} + 3540401664x^{38} + 89636864x^{39} - 238178304x^{40} - 90902528x^{41} - 3194880x^{42},
\end{aligned}
$$

$$
\begin{aligned}
q_6(x) &= 1-50x-1632x^2-3256x^3+195793x^4+1340389x^5-7988940x^6-67894229x^7+119798781x^8\\
&+1062782154x^9-2235428110x^{10}-3262969067x^{11}+37596694328x^{12}-37252689872x^{13}\\
&-297562909349x^{14}+236210791031x^{15}+1340218677244x^{16}-1251017551720x^{17}\\
&-4074480131076x^{18}+5117424381228x^{19}+9751997894756x^{20}-13887779309408x^{21}\\
&-17317172529164x^{22}+23032611039284x^{23}+21391658508296x^{24}-25887837535464x^{25}\\
&-16642696145344x^{26}+21644490331056x^{27}+5293706788512x^{28}-9977388037824x^{29}\\
&+626565257952x^{30}+1008822592320x^{31}-170655245632x^{32}+626889876736x^{33}\\
&-136651670784x^{34}-200545743872x^{35}+23315666944x^{36}+24227677184x^{37}+3305501184x^{38}\\
&-710127616x^{39}-924273664x^{40}-28921856x^{41}+41058304x^{42}+1597440x^{43},
\end{aligned}
$$

$$
\begin{aligned}
r_6(x) &= 85-2203x+35439x^2-392325x^3+2421300x^4-13948455x^5+52614679x^6-181382946x^7\\
&+457889661x^8-1051922025x^9+1785351655x^{10}-4053888558x^{11}+4573499148x^{12}\\
&-14264848622x^{13}+12026937315x^{14}-36446441384x^{15}+18329034236x^{16}-57637177788x^{17}\\
&-16153664292x^{18}-24803139708x^{19}-99171922408x^{20}+30377348160x^{21}\\
&-70760629468x^{22}+14910670192x^{23}-19424170912x^{24}-52979205872x^{25}+29465417632x^{26}\\
&-31307164896x^{27}+9736432704x^{28}-6425231264x^{29}-955152128x^{30}-2233139072x^{31}\\
&-1234877568x^{32}-152301824x^{33}-221951232x^{34}-56185344x^{35}-9267200x^{36}\\
&-1609216x^{37}+973824x^{38}+12288x^{39},
\end{aligned}
$$

$$
\begin{aligned}
s_6(x) &= 1-3x+509x^2-11751x^3+89334x^4-701193x^5+2868499x^6-12775076x^7+35485215x^8\\
&-97834113x^9+213752857x^{10}-428760104x^{11}+579275658x^{12}-1899415958x^{13}\\
&+1130367475x^{14}-7258329632x^{15}+1356473226x^{16}-15324003064x^{17}-10351491120x^{18}\\
&-30185827716x^{19}-31847892184x^{20}-17529900952x^{21}-39250822876x^{22}\\
&-9524944368x^{23}-9711493464x^{24}-7661892288x^{25}-18553132432x^{26}-18319877120x^{27}\\
&+10033361376x^{28}-3049287584x^{29}-2018893696x^{30}-1822695616x^{31}-453180800x^{32}\\
&-238571264x^{33}-296170496x^{34}-52508160x^{35}-14921216x^{36}-5137920x^{37}\\
&-406528x^{38}-500736x^{39}-6144x^{40}.
\end{aligned}
$$

Since $\deg(q_6) = 43$, we deduce that $t_6(n)$ satisfies a linear homogeneous recurrence relation of order 43. Similarly, $t_6^{nc}(n)$ and $t_6^{c}(n)$ are both of order 83, their first twelve values of $t_6^{nc}(n)$ and $t_6^{c}(n)$ are listed in Table 5.

6.6. Thin triangular grid cylinder for $7 \le m \le 10$

For $m = 7$, we find $q_7(x)$ divides $q_7^{nc}(x) = q_7^{c}(x)$. Since $\deg(q_7) = 116$, and $\deg(q_7^{nc}) = 226$, we conclude that $t_7(n)$ satisfies a linear homogeneous recurrence relation of order 116, and $t_m^{nc}(n)$ and $t_m^{c}(n)$ are of order 226.

Due to their complexity, we shall not display the generating functions for $m \ge 7$. We compile the first twelve values of $t_m^{nc}(n)$ and $t_m^{c}(n)$ for $6 \le m \le 8$ in Table 5, and the first ten values for $9 \le m \le 10$ in Table 6.

6.7. Validation of the computational results

The results presented above have been confirmed by an independent computation of the sum $t_m^{nc}(n) + t_m^{c}(n)$ $(2 \le m \le 10)$ using the standard method (see, for example, [11]) of enumerating HC over the vertices of a graph.

n	$t_6^{nc}(n)$	$t_6^{c}(n)$
1	98	12
2	1508	3456
3	171010	184680
4	13596692	12039660
5	922336108	938770020
6	67099253228	67882044840
7	4909187089576	4885209856092
8	355376976496136	355241907635520
9	25770442378940944	25788868513221612
10	1870551473132732576	1870339903143995736
11	135715037935252222288	135706060688950237656
12	9846357494694583886300	9846648051804937904760

n	$t_7^{nc}(n)$	$t_7^{c}(n)$
1	211	14
2	5054	13580
3	1313578	1487206
4	232545922	198694720
5	33189410002	33768467110
6	5153607780202	5241320047852
7	809663908291714	804827198825846
8	125424684761724236	125307843823985732
9	19460412645062644976	19479748508044269704
10	3023935942411311584398	3023653167447605305452
11	469636123603097988647768	469584019968079409562498
12	72931387395038191118319024	72934049510581997949471988

n	$t_8^{nc}(n)$	$t_8^{c}(n)$
1	453	16
2	17156	52224
3	9997336	11775328
4	3896059336	3223417488
5	1167155913080	1185621756624
6	384798689792288	393135995007392
7	129111358349224728	128238416460839040
8	42595006909351408208	42531816124977363184
9	14071165745328257792040	14088190273380013246144
10	4657567370179792834264272	4657291086796792759487616
11	1540753295054499621095480664	1540521771845487850011448176
12	509619452751384459772745689008	509639518558056304253948981168

Table 5. The first twelve values of $t_m^{nc}(n)$ and $t_m^{c}(n)$ for $6 \leq m \leq 8$.

n	$t_9^{nc}(n)$	$t_9^{c}(n)$
1	973	18
2	58056	197712
3	75624978	91604862
4	64223715600	51409628640
5	40221958446966	40802612538942
6	28065440384956200	28782720220289760
7	20031451724331532734	19877438499197428566
8	14021060961928795626528	13993475718821332020048
9	9826062975710517676318602	9839825848777598512393806
10	6902704293045726186844650096	6902426210533756839116417196

n	$t_{10}^{nc}(n)$	$t_{10}^{c}(n)$
1	2090	20
2	196288	739280
3	570206046	704216720
4	1048198919132	809477044320
5	1367718687127664	1384316446458200
6	2013931487585742288	2072057339935694660
7	3048855545115197548 29	3021870581641678162000
8	4514966409171605952717452	4503652523011415867218000
9	6694060137695157532017399784	6704544346009821140767285260
10	9952972682436734575332405583708	9952625171775890838486704218360

Table 6. The first ten values of $t_m^{nc}(n)$ and $t_m^{c}(n)$ for $9 \le m \le 10$.

7. Asymptotic Relations and an Open Problem

We can write

$$\mathcal{T}_m^{nc}(x) = \overline{\mathcal{T}^{nc}}_m(x) + \frac{u_m^{nc}(x)}{w_m(x)} \quad \text{and} \quad \mathcal{T}_m^{c}(x) = \overline{\mathcal{T}^{c}}_m(x) + \frac{u_m^{c}(x)}{w_m(x)},$$

for some polynomials $\overline{\mathcal{T}^{nc}}_m(x)$, $\overline{\mathcal{T}^{c}}_m(x)$, $u_m^c(x)$, $u_m^{nc}(x)$ and $w_m(x)$, such that $\deg(u_m^{nc})$, $\deg(u_m^c) < \deg(w_m)$. Obviously, $w_m(x) = q_m(x)s_m(x)$. Valuable information about $t_m^{nc}(n)$ and $t_m^c(n)$ can be obtained from the rational functions $u_m^{nc}(x)/w_m(x)$ and $u_m^c(x)/w_m(x)$. For example, both sequences satisfy a linear recurrence relation whose characteristic polynomial is $\psi_m(t) = t^{\delta_m} w_m(1/t)$, where $\delta_m = \deg(w_m)$. Let the roots of $\psi_m(t)$ be $\lambda_{m,i}$, where $1 \le i \le \delta_m$. If they are distinct, then

$$\frac{u_m^{nc}(x)}{w_m(x)} = \prod_{i=1}^{\delta_m} \frac{\alpha_i}{1 - \lambda_{m,i} x},$$

where $\alpha_i = -\lambda_{m,i} u_m^{nc}(\lambda_{m,i}^{-1})/w_m'(\lambda_{m,i}^{-1})$. Hence, for sufficiently large n,

$$t_m^{nc}(n+1) = \sum_{i=1}^{\delta_m} \alpha_i \lambda_{m,i}^n.$$

The solution is more complicated if some of the $\lambda_{m,i}$s are repeated roots. Nonetheless, if one of the roots, say $\lambda_{m,1}$, is a simple positive root which is greater than the moduli of all other roots, then $\lambda_{m,1}$ is the dominant root, and

$$t_m^{nc}(n+1) \sim \alpha_1 \lambda_{m,1}^n,$$

in which the formula for α_1 given above still holds. We find that such a dominant root exists for $2 \le m \le 7$. Is it always true? We believe it is. To support our argument, let us study the matrix T_m^*.

Note that the $\lambda_{m,i}$s are the characteristic roots of the transfer matrix T_m^*. Let $\overline{T}_m^*$ be the matrix obtained from T_m^* by deleting the row and the column corresponding to the isolated vertex v^*. We find that, for $2 \le m \le 7$, the matrix $\overline{T}_m^* + (\overline{T}_m^*)^2 + (\overline{T}_m^*)^3 + (\overline{T}_m^*)^4$ is positive. Therefore, the multidigraph $\mathcal{D}_m^* - v^*$ is strongly connected; in other words, $\overline{T}_m^*$ is irreducible. In addition, loops exist in $\mathcal{D}_m^* - v^*$, because, for instance, the first two columns of B could be the word $(2\text{-}2, 0\text{-}0, 3\text{-}3, 0\text{-}0, \ldots, (\ell+1)\text{-}(\ell+1), 0\text{-}0)$ when $m = 2\ell$, or the word $(2\text{-}2, 0\text{-}0, 3\text{-}3, 0\text{-}0, \ldots, (\ell+1)\text{-}(\ell+1), 0\text{-}0, 0\text{-}2)$ when $m = 2\ell+1$. We conclude that $\overline{T}_m^*$ is primitive (see, for example, [12]). It follows from the Perron-Frobenius Theory that $\overline{T}_m^*$ has a positive eigenvalue θ_m (what we called $\lambda_{m,1}$ above) such that $\theta_m > |\mu|$ for any other eigenvalue μ. Then

$$t_m^{nc}(n+1) \sim a_m \theta_m^n,$$

for some positive number a_m. In fact, $a_m = -\theta_m u_m^{nc}(\theta_m^{-1})/w_m'(\theta_m^{-1})$. Likewise,

$$t_m^{c}(n+1) \sim b_m \theta_m^n,$$

where $b_m = -\theta_m u_m^{c}(\theta_m^{-1})/w_m'(\theta_m^{-1})$. Numerical data confirm that $a_m = b_m$ for $2 \le m \le 7$. See Table 7, in which we also list the entropy (see Section 1) per site:

$$\lim_{n\to\infty} \frac{\ln t_m(n)}{m(n+1)} = \ln \sqrt[m]{\theta_m}.$$

The observation that $a_m = b_m$ for $2 \le m \le 7$ leads to the following conjecture.

Conjecture 6. *For each integer $m \ge 2$, $\lim_{n\to\infty} t_m^{nc}(n)/t_m^{c}(n) = 1$.*

There are many other related problems that one can explore. If these two numbers $t_m^{nc}(n)$ and $t_m^{c}(n)$ are indeed asymptotically equal, can we identify, based

on the homotopy, the subsets of these two types of HCs that are equinumerous asymptotically. Alternatively, can we characterize the homotopic structures of those HCs that make $t_m^{nc}(n) \neq t_m^c(n)$? Can such a difference be linked to the critical indices (or critical exponents) studied in theoretical physics?

m	θ_m	$a_m = b_m$	$\sqrt[m]{\theta_m}$
2	2.000000	4.000000	1.414214
3	6.872983	6.654738	1.901290
4	15.240430	10.859483	1.975829
5	33.442423	19.535467	2.017714
6	72.555179	33.568305	2.042262
7	155.304851	57.529046	2.056016

Table 7. The approximate values of θ_m, a_m and $\sqrt[m]{\theta_m}$.

Acknowledgment

The authors are indebted to the anonymous referee for his/her valuable suggestions and the reference [9]. The comments help us improve the exposition in this article.

References

[1] O. Bodroža-Pantić, B. Pantić, I. Pantić and M. Bodroža-Solarov, *Enumeration of Hamiltonian cycles in some grid graphs*, MATCH Commun. Math. Comput. Chem. **70** (2013) 181–204.

[2] O. Bodroža-Pantić, H. Kwong and M. Pantić, *Some new characterizations of Hamiltonian cycles in triangular grid graphs*, Discrete Appl. Math. **201** (2016) 1–13. doi:10.1016/j.dam.2015.07.028

[3] O. Bodroža-Pantić, H. Kwong and M. Pantić, *A conjecture on the number of Hamiltonian cycles on thin grid cylinder graphs*, Discrete Math. Theoret. Comput. Sci. **17** (2015) 219–240.

[4] O. Bodroža-Pantić and R. Tošić, *On the number of* 2*-factors in rectangular lattice graphs*, Publ. Inst. Math. (Beograd) (N.S.) **56** (1994) 23–33.

[5] D.M. Cvetković, M. Doob and H. Sachs, Spectra of Graphs: Theory and Application (VEB Deutscher Verlag der Wissenschaften, Berlin, 1982).

[6] F.J. Faase, *On the number of specific spanning subgraphs of the graphs* $G \times P_n$, Ars Combin. **49** (1998) 129–154.

[7] M.J. Golin, Y.C. Leung, Y. Wang and X. Yong, *Counting structures in grid-graphs, cylinders and tori using transfer matrices: survey and new results* (extended abstract), in: Proceedings of SIAM ALENEX/ANALCO Workshop—Analytic Algorithmics and Combinatorics (Canada, 2005), 250–258.

[8] J.L. Jacobsen, *Exact enumeration of Hamiltonian circuits, walks and chains in two and three dimensions*, J. Phys. A **40** (2007) 14667–14678. doi:10.1088/1751-8113/40/49/003

[9] I. Jensen, *Self-avoiding walks and polygons on the triangular lattice*, J. Stat. Mech. Theory Exp. (2004) P10008. doi:10.1088/1742-5468/2004/10/P10008

[10] A.M. Karavaev, *Kodirovanie sostoyanĭi v metode matricy perenosa dlya podscheta gamil'tonovyh ciklov na pryamougol'nyh reshetkah, cilindrah i torah*, Informacionnye Processy **11** (2011) 476–499 (in Russian).

[11] A. Karavaev and S. Perepechko, *Counting Hamiltonian cycles on triangular grid graphs*, IV International Conference (Kiev, 2012).

[12] B.P. Kitchens, Symbolic Dynamics: One-sided, Two-sided and Countable State Markov Shifts (Springer, 1997).

[13] G. Kreweras, *Dénombrement des Cycles Hamiltoniens dans un Rectangle Quadrillé*, European J. Combin. **13** (1992) 473–467. doi:10.1016/0195-6698(92)90005-K

[14] Y.H.H. Kwong, *Enumeration of Hamiltonian cycles in $P_4 \times P_n$ and $P_5 \times P_n$*, Ars Combin. **33** (1992) 87–96.

[15] Y.H.H. Kwong and D.G. Rogers, *A matrix method for counting Hamiltonian cycles on grid graphs*, European J. Combin. **15** (1994) 277–283. doi:10.1006/eujc.1994.1031

[16] M. Peto, T.Z. Sen, R.L. Jernigan and A. Kloczkowski, *Generation and enumeration of compact conformations on the two-dimensional triangular and three-dimensional fcc lattices*, J. Chem. Phys. **127** (2007) Article 044101.

[17] T.G. Schmalz, G.E. Hite and D.J. Klein, *Compact self-avoiding circuits on two dimensional lattice*, J. Phys. A **17** (1984) 445–453. doi:10.1088/0305-4470/17/2/029

[18] R.P. Stanley, Enumerative Combinatorics, Vol. I (Cambridge University Press, Cambridge, 2002).

[19] R. Stoyan and V. Strehl, *Enumeration of Hamiltonian circuits in rectangular grids*, J. Combin. Math. Combin. Comput. **21** (1996) 109–127.

[20] R. Tošić, O. Bodroža, Y.H.H. Kwong and H.J. Straight, *On the number of Hamiltonian cycles of $P_4 \times P_n$*, Indian J. Pure Appl. Math. **21** (1990) 403–409.

Received 1 April 2016
Revised 20 October 2016
Accepted 5 December 2016